J. Meas. Sci. Instrum., 2025, 16(2): 224-235. http://jmsi.publish.founderss.cn
DOI: 10.62756/jmsi.1674-8042.2025022 jmsi@nuc.edu.cn

Typical electrode discharge acoustic signal denoising in oil based on improved VMD

CAO Panpan[1], MA Jianqiao[1*], YANG Guangze[1], FENG Tingna[2], WANG Xin[3]

1. School of Automation and Electrical Engineering, Lanzhou Jiaotong University, Lanzhou 730070, China;
2. Hami Power Supply Company of State Grid Xinjiang Electric Power Co., Ltd., Hami 839000, China;
3. Baotou Power Supply Bureau, Inner Mongolia Electric Power (Group) Co., Ltd., Baotou 014030, China

***Corresponding author:** MA Jianqiao (lzjdmjq@163.com)

Received: October 21, 2023 **Revised:** December 13, 2023 **Accepted:** January 15, 2024

Abstract: In order to suppress the white noise interference in partial discharge (PD) detection and accurately extract the characteristics of local discharge pulse acoustic signal of transformer under strong noise environment, the adaptive separation and denoising of the discharge pulse acoustic signal were analyzed under low signal-to-noise ratio (SNR) environment. Firstly, the optimal decomposition mode number K of the variational mode decomposition (VMD) was determined based on Spearman correlation coefficient, then the reliability of the proposed Spearman-variational mode decomposition (SVMD) method decomposition was verified by simulated signals, and finally the actual discharge pulse acoustic signal was decomposed and denoised based on the Spearman correlation coefficient averaging threshold method to extract the eigenmode function components of the discharge pulse signal. The results showed that SVMD adaptively solved the unknown defects of VMD mode number, and effectively extracted the modal components of complex signals, and successfully realized the denoising of transformer partial discharge acoustic signals. The proposed method effectively removed white noise interference in the partial discharge acoustic signal and obtained a smooth filtered signal. It retained the integrity of the partial discharge signal to the maximum extent and was beneficial to the subsequent research of partial discharge. The improvement of VMD was helpful to promote its wide use in industrial equipment condition inspection.

Key words: failure recognition; Spearman correlation coefficient; variational mode decomposition (VMD); partial discharge; acoustic signal

0 Introduction

Partial discharge (PD) is the initial sign and manifestation of insulation degradation in transformers[1,2]. The defects of internal transformer such as impurities in oil, air bubbles, and mechanical manufacturing lead to an over-concentration of field intensity in the local area of the transformer inducing electric field distortion, which generates partial discharge, increasing the risk of failure[3,4].

Transformer partial discharge caused by the sound signal belongs to the measurement of transient weak pulse signal. The field testing environment of substation is complicated, the transformer operating environment is bad, and there are many noise sources around. At the same time, there are many different types of electromagnetic interference, and most of the transformer operation acoustic signals collected at the substation site contain a large amount of mixed noise, which affects the detection effect and brings serious interference to fault identification, especially the white noise interference is the most serious[5]. Therefore, white noise removal is essential in transformer fault diagnosis research. The commonly used denoising methods are Fourier transform, wavelet transform[6], empirical mode decomposition (EMD)[7], and the subsequent proposed variational mode decomposition, etc. Fourier transform is suitable for processing linear and smooth signals. Wavelet transform is a widely used noise reduction method. However, since the number of decomposition layers and the wavelet basis function of the adapted signal need to be preset before denoising, it brings artificial interference and cannot be adaptively denoised.

The proposed variational modes have a complete theoretical basis after decomposition[8], and avoid the difficulties of recursive modes, modal confusion, end effects, and similar frequency separation in empirical mode decomposition. Moreover, the VMD algorithm is more robust to noise and sampling, so it has been successfully used for denoising signals in fields such as biology[9], seismic[10], and acoustics[11].

However, before using the VMD method, some algorithm parameters need to be set. The most important one is the decomposition mode number K. It affects the effectiveness of denoising. It is crucial to choose the exact value of K before VMD denoising. The parameter K specifies how many intrinsic mode functions (IMFs) can be separated by VMD. When K is small, it cannot decompose enough mode components, which will easily cause multiple mode components to be concentrated in one mode function, called mixed mode, and it will also lead to transient center frequency vibration non-constant phenomenon. When K is larger, more modes need to be decomposed. This results in a modal component being decomposed into different modes, i. e., modal redundancy. It will increase the computational pressure and reduce the efficiency of the system.

The traditional K value selection is an iterative process, which is time consuming and leads to unreliable results. K value selection has been studied, but the results are relatively few and the implementation process is complicated and tedious, such as the de-trended fluctuation analysis method[12], central frequency method[13], kurtosis maximum method[14], the instantaneous frequency mean method[15], the EMD method[16], and intelligent parameter optimization method[17]. These methods lack clear parameter criteria in the actual decomposition process and have a large subjective influence, and the methods are becoming more and more complex, such as genetic algorithm to find the best[18]. Fu used fruit fly algorithm to optimize the two parameters of K and α of VMD[19]. Wang used artificial bee colony algorithm to optimize VMD algorithm to process gear vibration signal[20].

In addition, when using VMD denoising, it is very important to extract the effective eigenmode function after decomposing the noise-containing signal. Some difficulties are faced, such as the complexity of signal component crossing, the unknown characteristics of noisy signals, and the loss of effective signal features due to incomplete or excessive de-noising. Especially in complex signals, the effective signal characteristics cannot be determined in advance, and the noise and effective signal components cannot be distinguished when denoising, which brings great challenges to the effective signal feature extraction.

A VMD decomposition method was proposed based on Spearman correlation coefficient improvement, that was Spearman-variational mode decomposition (SVMD). Firstly, the original signal was decomposed by VMD based on Spearman correlation coefficient improvement to determine the optimal decomposition mode number K. And then the reliability of the method decomposition was verified by simulated signals. Finally, the effective signal components after VMD decomposition were selected according to the correlation coefficient threshold method to achieve the suppression of white noise in a low signal-to-noise ratio environment. It was successfully applied to the study of the denoising of transformer partial discharge acoustic signal. The results showed that the method effectively removed white noise interference and obtained a smooth filtered signal, which retained the integrity of PD signal to the maximum extent and was beneficial to the subsequent study of partial discharge. Its improvements help to promote its wide application in condition monitoring of industrial equipment.

The innovations of the SVMD denoising method were as follows. First of all, whether it was an simulation signal or an actual PD sound signal, SVMD could be effectively adaptively decomposed. The signal had a wide range of applications and was more advantageous for the discharge pulse signal. This was determined by the characteristics of the VMD decomposition method itself. Compared with the wavelet denoising and decomposition, SVMD method was not necessary to select the applicable wavelet basis function in advance. Secondly, based on the Spearman correlation coefficient of the noisy original signal and the reconstructed signal, the adaptive selection of the K value in the VMD method could be realized, which improved the previous human experience analysis error and avoided over-decomposition and modal mixing defects. In addition, the VMD decomposition K value correction of complex signals could be realized through the Spearman correlation coefficient. The Spearman correlation coefficient of the K value was optimized to make it return to the best state. Finally, when the K value in the VMD decomposition was determined, the noise component could be eliminated by the average threshold of the Spearman correlation coefficient among the K IMFs components and the original signal. Compared with wavelet denoising, SVMD denoising was conducive to extracting the characteristics of each component in the original signal, and had a more thorough understanding of the signal, which was convenient for subsequent PD identification research.

1 SVMD denoising principle

1.1 VMD

VMD estimates the individual signal components by solving a frequency domain variational optimization problem. Assuming that all components are narrowband signals concentrated around their respective center frequencies, VMD constructs a constrained optimization problem based on the component narrowband condition to estimate the center frequencies of the signal components and reconstruct the corresponding components. VMD decomposition can decompose complex signals into several intrinsic mode component sub-sequences, namely IMF, where the decomposed signal is the same as the sum of the modes[8]. Assuming that the signal $f(t)$ consists of K natural mode components and each natural mode component can be defined as an FM/AM signal. $u_k(t)$ ($k=1,\cdots,K$) can be expressed as

$$u_k(t)=A_k(t)\cos\left[\varphi_k(t)\right], \tag{1}$$

where $A_k(t)$ ($k=1,\cdots,K$) is the amplitude of $u_k(t)$ and $A_k(t)\geqslant 0$; $\varphi_k(t)$ ($k=1,\cdots,K$) is the phase of $u_k(t)$. The instantaneous frequency $\omega_k(t)$ ($k=1,\cdots,K$) of $u_k(t)$ is obtained by

$$\omega_k(t)=\frac{\mathrm{d}\varphi_k(t)}{\mathrm{d}t}. \tag{2}$$

For the variational modal problem of constructing the signal $f(t)$, solving the Hilbert transform for the one-sided spectrum of each $u_k(t)$ yields the analytic signal corresponding to each $u_k(t)$ as

$$\left(\delta(t)+\frac{\mathrm{j}}{\pi t}\right)u_k(t), \tag{3}$$

where δ(t) denotes the unit pulse function. The resolved signal corresponding to each $u_k(t)$ signal plus the correction factor $\mathrm{e}^{-\mathrm{j}\omega_k t}$ modulates the spectrum of each $u_k(t)$ to its corresponding fundamental frequency. The corresponding demodulated signal is obtained by

$$\left[\left(\delta(t)+\frac{\mathrm{j}}{\pi t}\right)u_k(t)\right]\mathrm{e}^{-\mathrm{j}\omega_k t}. \tag{4}$$

The gradient squared L^2 parametrization of Eq. (4) is calculated to obtain the bandwidth of $u_k(t)$. Using the bandwidth, the corresponding constrained variational problem can be constructed by

$$\begin{aligned}&\min_{\{u_k\}\{\omega_k\}}\left\{\sum_{k=1}^{K}\left\|\partial_t\left[\left(\delta(t)+\frac{\mathrm{j}}{\pi t}\right)*u_k(t)\right]\mathrm{e}^{-\mathrm{j}\omega_k t}\right\|_2^2\right\},\\&\text{s.t.}\sum_{k=1}^{K}u_k(t)=f(t),\end{aligned} \tag{5}$$

where u_k denotes the K IMF components obtained from the VMD decomposition; ω_k denotes the central frequency of the IMF components; $*$ denotes the convolution operation; ∂_t denotes the derivative of the function with respect to time; and δ(t) is the unit impulse function. Eq. (5) is transformed into an unconstrained variational problem and its optimal solution is found. In order to ensure the accuracy of signal reconstruction under Gaussian noise, a quadratic penalty factor α is introduced, and a Lagrangian operator λ is introduced to ensure the strictness of the constraints in the solution process. Thus the augmented Lagrangian expression is

$$\begin{aligned}&L(\{u_k\},\{\omega_k\},\lambda)=\\&\alpha\sum_{k=1}^{K}\left\|\partial_t\left[\left(\delta(t)+\frac{\mathrm{j}}{\pi t}\right)*u_k(t)\right]\mathrm{e}^{-\mathrm{j}\omega_k t}\right\|_2^2+\\&\left\|f(t)-\sum_{k=1}^{K}u_k(t)\right\|_2^2+\left\langle\lambda(t),f(t)-\sum_{k=1}^{K}u_k(t)\right\rangle,\end{aligned} \tag{6}$$

where u_k^{n+1}, ω_k^{n+1}, and λ_k^{n+1} are continuously updated alternately with each other, so as to find the saddle point of Eq. (6), that is the optimal solution of Eq. (5). The expressions that update the variable during iteration are

$$\begin{aligned}&\hat{u}_k^{n+1}(\omega)=\frac{\hat{f}(\omega)-\sum_{k=1}^{K}\hat{u}_k(\omega)+\frac{\hat{\lambda}(\omega)}{2}}{1+2\alpha(\omega-\omega_k)^2},\\&\omega_k^{n+1}=\frac{\int_0^{\infty}\omega\left|\hat{u}_k(\omega)\right|^2\mathrm{d}\omega}{\int_0^{\infty}\left|\hat{u}_k(\omega)\right|^2\mathrm{d}\omega},\\&\hat{\lambda}^{n+1}(\omega)=\hat{\lambda}^{n}(\omega)+\tau\left[\hat{f}(\omega)-\sum_{k=1}^{k}\hat{u}_k^{n+1}(\omega)\right],\end{aligned} \tag{7}$$

where $\hat{u}_k^{n+1}(t)$ denotes the Wiener filter of the current residual; ω_k^{n+1} denotes the center frequency of the power spectrum of the current mode function, and then the Fourier inversion of $\{u_k(\omega)\}$ is performed to take the real part to obtain the time-domain mode component $\{u_k(t)\}$.

1.2 Improved VMD

The Spearman correlation coefficient is a test method independent of the data distribution and is more suitable for dealing with abruptly changing state acoustic signals in complex environments[21]. It can be used to assess the relationship between two variables and can be described by using monotonic functions. As with any correlation coefficient calculation, Spearman correlation coefficient is applicable to continuous[22], discrete, and ordinal variables, and it is often described as a nonparametric characteristic. For the original data x_i ($i=1,\cdots,n$) and y_i ($i=1,\cdots,n$) of size n, their ranks are rgx_i and rgy_i. The Spearman correlation coefficient r_s is calculated by

$$r_s=\frac{\mathrm{cov}(rgx_i,rgy_i)}{\sigma_{rgx_i}\sigma_{rgy_i}}, \tag{8}$$

where $\mathrm{cov}(rgx_i,rgy_i)$ is the covariance of the rank variables; σ_{rgx_i} and σ_{rgy_i} are the standard deviations of the rank variables.

Under 50 Hz and 300 Hz simulated signals, the variation characteristics of Spearman correlation coefficient between the reconstructed signal and the original signal were verified by VMD decomposition. Assuming that $K=1$ in VMD decomposition, K IMF component signals are obtained by VMD decomposition. And then, according to VMD decomposition principle $f(t)=\sum_{k=1}^{K} u_k(t)$, the reconstructed signal is obtained. Calculate the Spearman correlation coefficient between the original signal and the reconstructed signal, and finally determine whether the Spearman correlation coefficient is greater than or equal to 1. If the group is not satisfied, then $K=K+1$, repeat the above process. If it is satisfied, the calculation is terminated and the K value in this data is kept at this time.

The Spearman correlation coefficient between the reconstructed sequence and the original sequence in Fig.1 can be obtained with the variation process of the K value of the VMD decomposition. The data in Fig. 1 shows that as the number of decomposition modes K increases, the Spearman correlation coefficient between the reconstructed sequence and the original sequence will continue to increase. When the signal is completely decomposed, with the increase of K, the Spearman correlation coefficient gradually tends to be stable.

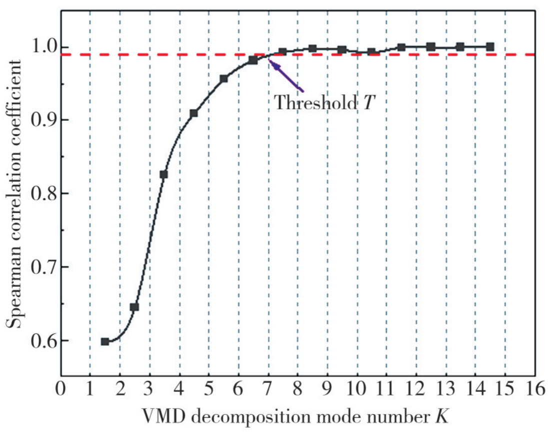

Fig. 1 Trend of Spearman correlation coefficient with number of VMD decomposition modes *K*

Therefore, when the Spearman correlation coefficient between the original signal and the reconstructed signal reaches the threshold, it can be considered that the signal has been sufficiently decomposed by VMD. Through several denoising experiments on simulation signals and partial discharge acoustic signals, it is found that when the Spearman correlation coefficient between the reconstructed signal and the original signal is 0.996, the SVMD method has the best denoising effect, so the ideal threshold T is set as 0.996.

In VMD decomposition, the decomposition mode number K is the main parameter of the VMD denoising method. Different K will directly lead to the difference in the IMF components after VMD decomposition. The other parameters in the VMD method will also have denoising effects. Only the decomposition mode number K is discussed. Therefore, the default options are kept for the remaining related parameters in the VMD method, and only the K value is changed in multiple decompositions, among which, the PenaltyFactor=1 000, LMUpdateRate=0.01 and MaxIterations=500.

2 Simulation signal verification

In order to verify the adaptive separation effect of the proposed SVMD method, this paper illustrates the detailed separation process and verifies its reliability by simulating the signal, generating continuous smooth signal through MATLAB. $f_1=50$ Hz and $f_2=300$ Hz can be specified, according to the sampling law signal sampling frequency $f_s=1\,000$ Hz. The simulated signal can be expressed as

$$f(t)=\cos(2\pi f_1 t)+2\cos(2\pi f_2 t)+n(t), \qquad (9)$$

where $n(t)$ is the Gaussian white noise signal with different signal-to-noise ratios added. The generated simulation signal is shown in Fig. 2, which is the time domain waveform of the simulation signal after adding 10 dB white noise. It is obvious that the signal waveform is slightly distorted after adding white noise, and no more useful feature information can be obtained from the time domain. So it turns to the frequency domain features, the results are shown in Fig.2(b). The frequency distribution shows that the original signal contains a large number of 50 Hz and 300 Hz signals. And there is white noise interference distributed throughout the signal frequency band.

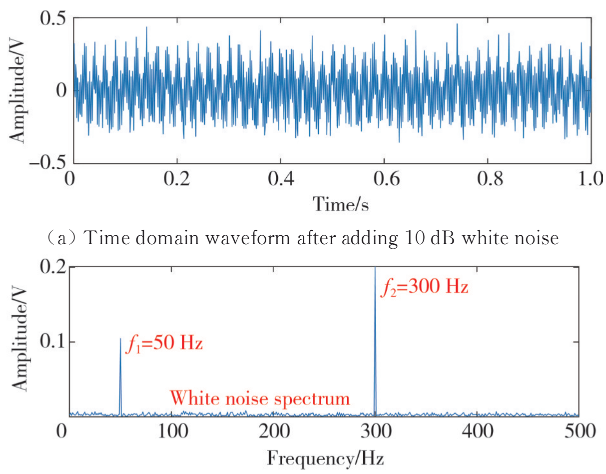

(b) Frequency domain characteristics after adding 10 dB white noise

Fig. 2 Time-frequency spectrogram

2.1 K value determination by SVMD method

At this point, the simulation signal needs to be decomposed to extract the 50 Hz and 300 Hz signal components, and the detailed process of determining the optimal mode number for SVMD is as follows.

Step 1 Assume that the decomposition mode number $K=1$, then the original signal $f(t)$ is decomposed by VMD to obtain the initial K IMF components.

Step 2 Solve the K IMF component reconstruction signal $\hat{f}(t)$ according to $f(t)=\sum_{k=1}^{K} u_k(t)$.

Step 3 Calculate the Spearman correlation coefficients of the original signal $f(t)$ and the reconstructed signal $\hat{f}(t)$.

Step 4 Determine whether the Spearman correlation coefficient obtained in step 3 is greater than or equal to 0.996. If it is less than 0.996, make $K=K+1$, and then repeat steps 2, 3, and 4 to continue the decomposition. If it is greater than or equal to 0.996, the value of K is the best decomposition mode number at this time.

For the simulation signal decomposed by SVMD, the Spearman correlation coefficients of the reconstructed signal and the original signal at different K values are shown in Table 1. And the optimal decomposition mode number K can be determined as 5. At this time, the waveform of each IMF component signal after the simulation signal decomposed by 5 layers is shown in Fig.3.

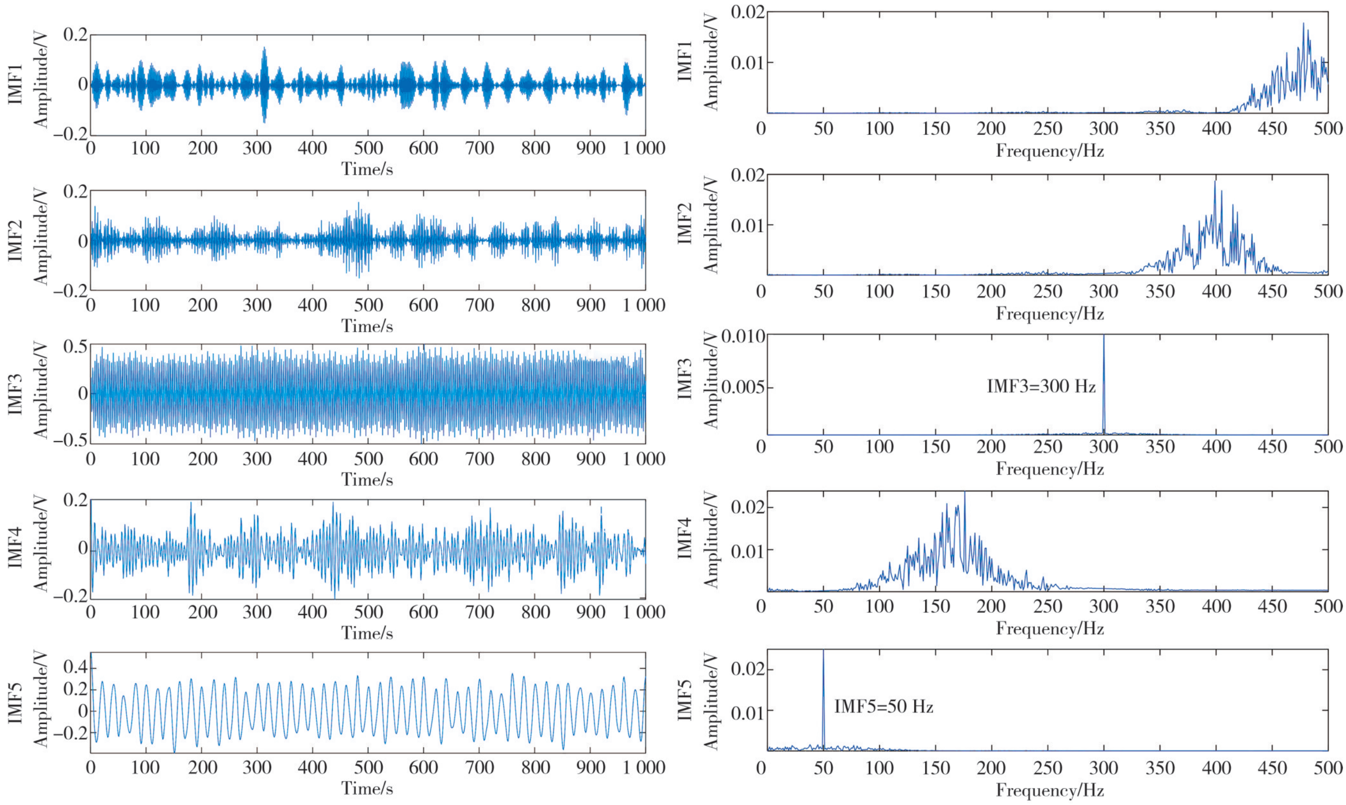

(a) IMF components after SVMD decomposition (b) Frequency distribution corresponding to each IMF component

Fig. 3 Time-frequency characteristics of IMF components of simulation signals

Table 1 Spearman correlation coefficient of reconstructed signal and original signal

K	Spearman correlation coefficient
1	0.759 3
2	0.823 6
3	0.985 8
4	0.992 6
5	0.997 3

At this time, the simulation acoustic signal has been completely decomposed. The signal modes are independent of each other, and there is no interference. It can be seen from Fig. 3 that the time domain signal waveforms in the IMF3 and IMF5 components are stable and smooth, similar to the main information components in the original signal, and the rest each IMF component is interference information brought by white noise. The frequency distribution of each IMF signal decomposed by SVMD is calculated, and it can be found that the original signal frequency characteristics of 50 Hz and 300 Hz can be appeared, and there is no center frequency crossover phenomenon. So SVMD has completely decomposed the signal, and there will be no mode mixing problem. It can be seen that the proposed SVMD can improve the optimal modal number selection problem in the traditional VMD decomposition, and realize the complete decomposition of complex signals with the smallest operation process, and extract its effective signal components.

2.2 Verification and correction of *K* value of SVMD method

The improved VMD decomposition can well solve the problem of the optimal mode number of traditional VMD decomposition, and its decomposition is easy to realize for the simulation signal with known effective features, which can be verified by the inverse solution of known features to determine whether its decomposition is complete. However, the process is based on the known original signal frequency distribution and observation results, which has great subjective influence and cannot reasonably explain its reliability and validity. Therefore, it is necessary to further verify the rationality of the optimal *K* value of VMD decomposition based on the improved Spearman coefficient to prevent over-decomposition and under-decomposition.

In order to verify whether the preset *K* value of SVMD is optimal, the correlation analysis of each IMF component obtained from the decomposition of the *K* value determined by the decomposition optimization of SVMD is carried out. The correlation coefficient in each IMF component is used as a judgment index to check whether the preset *K* values are optimal. And it is also used to check whether there is over-decomposition or under-decomposition of the signal. The correlation coefficient between any two IMF components can correct the number of over-decomposed or under-decomposed IMF components of SVMD to obtain the optimal *K* value.

The test steps for determining the optimal *K* value using correlation coefficients are as follows.

Step 1 Adaptively decompose the original signal by SVMD to obtain the initially determined optimal decomposition *K* value.

Step 2 Based on the optimal *K* value determined by SVMD decomposition, the signal is then decomposed by VMD to obtain *K* IMF components.

Step 3 Perform correlation analysis on each IMF component and calculate the correlation coefficient between the IMF components.

Step 4 Determine whether there is over-decomposition of the components after SVMD decomposition. Over-decomposition means that the modal components of the same center frequency are decomposed into multiple IMF components with high correlation among their modal components. If the correlation coefficient value is less than 0.1, it is considered as the uncorrelated component. When over-decomposition occurs, the adjacent over-decomposed components with correlation coefficient values greater than 0.1 must be combined to obtain the final optimal *K* value after correction.

Step 5 When there is no over-decomposition component, it is necessary to verify whether there is under-decomposition phenomenon. Take the *K* value as $K+1$, perform the quadratic VMD decomposition of the signal, and judge whether there is an over-decomposition component in the decomposed IMF component. If there is an over-decomposition component, the optimal *K* value is considered to be *K*. Conversely, if there is no over-decomposition phenomenon, the *K* value cycle is taken as $K+n$ in turn, and n is the number of VMD decomposition cycles until the over-decomposition phenomenon occurs, then the optimal *K* value is $K+n-1$. The detailed decomposition state judgment process of VMD based on Spearman correlation coefficient is shown in Fig.4.

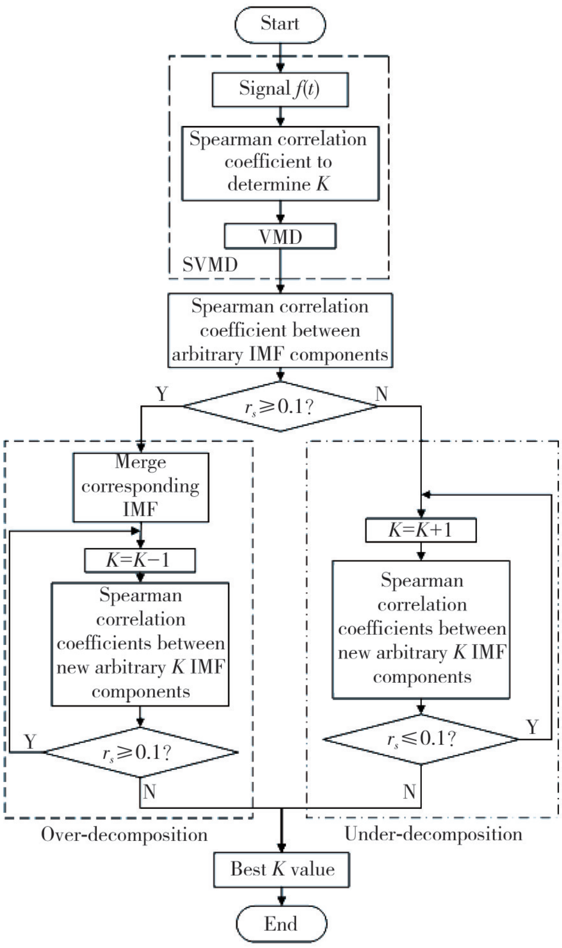

Fig. 4 Flow chart of VMD detailed decomposition state judgment based on Spearman correlation coefficient

The optimal decomposition *K* value is determined as 5 by SVMD decomposition, and the correlation coefficient is used to test its reliability. To check whether there is over-decomposition, the correlation coefficients between each IMF components when $K=5$ are shown in Table 2. It can be found that the correlation coefficient values among the IMF components are less than 0.1, which means that the IMF components are independent of each other and there is no over-decomposition phenomenon. At this point, the phenomenon of over-decomposition has been ruled out, but we also need to verify whether the decomposition is insufficient. The best decomposition value is given by SVMD when K value is 5. If the decomposition is insufficient, then we need to increase the K value, set $K=K+1$, so the K value is set to 6.

Table 2 Spearman correlation coefficient among IMFs (K=5)

IMF	Spearman correlation coefficient				
	IMF1	IMF2	IMF3	IMF4	IMF5
1	1				
2	0.098 1	1			
3	0.003 3	0.013 5	1		
4	0.011 1	0.025 4	0.009 5	1	
5	0.001 1	0.001 9	0.000 4	0.015 2	1

Observe the correlation coefficient value among the IMF components at this time. If there is a correlation coefficient value greater than 0.1, then the components are considered to be over-decomposition, and we need to roll back the K value to the previous state, and its correlation coefficient value is shown in Table 3.

Table 3 Spearman correlation coefficient among IMFs (K=6)

IMF	Spearman correlation coefficient					
	IMF1	IMF2	IMF3	IMF4	IMF5	IMF6
1	1					
2	0.097 1	1				
3	0.002 9	0.011 1	1			
4	0.011 3	0.028 1	0.015 1	1		
5	0.005 8	0.011 8	0.003 6	**0.118 1**	1	
6	0.000 6	0.001 2	0.000 2	0.005 2	0.019 8	1

The Spearman correlation coefficient values in the Table 3 reveal that the correlation coefficient value between IMF4 and IMF5 is greater than 0.1. Then IMF4 and IMF5 are over-decomposed components. Time-frequency characteristic diagram of simulation signal over-decomposition verification under white noise interference is shown as Fig. 5. It is found that the central frequency values of IMF4 and IMF5 are close to each other, thus leading to the phenomenon of over-decomposition. So it is necessary to roll back to the previous state. Since the period is 1, $K=K+n-1=5+1-1=5$, so the optimal number of decomposition modes is $K=5$.

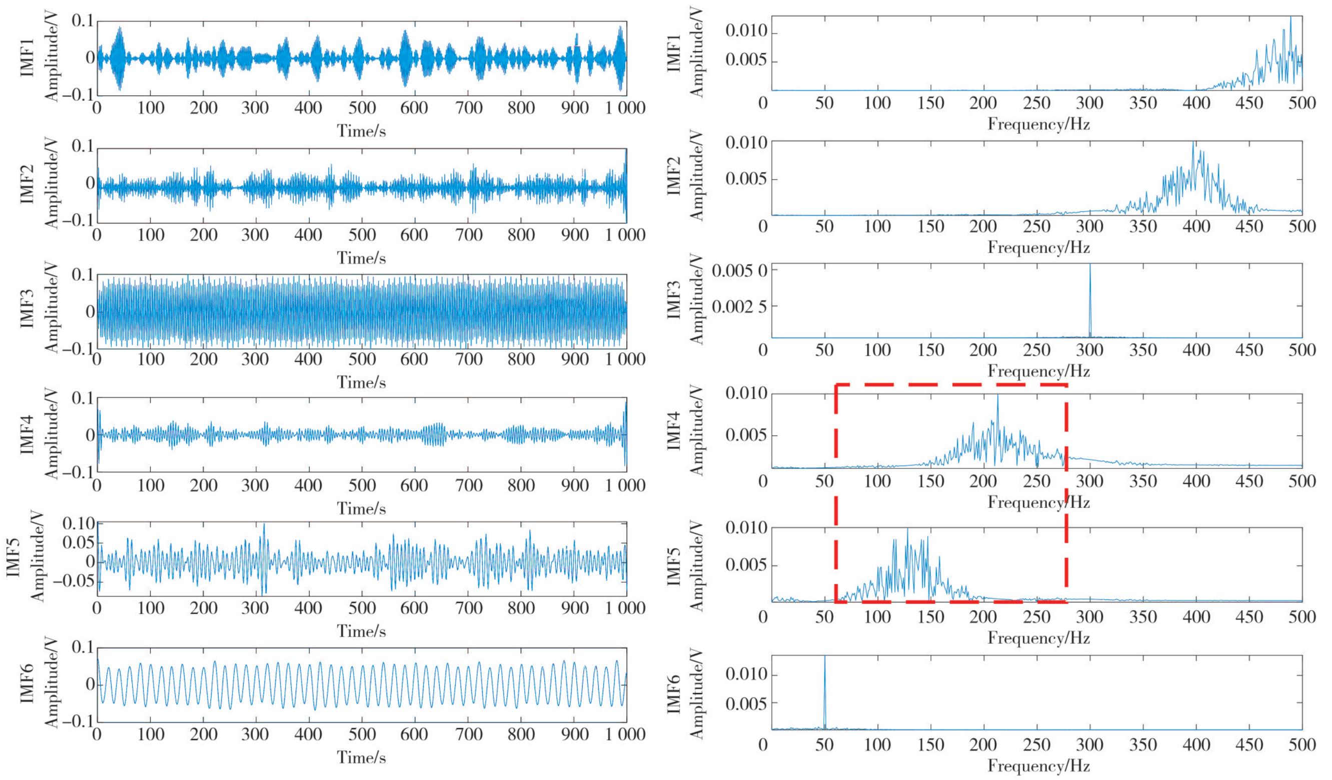

(a) IMF components after SVMD over-decomposition

(b) Frequency distribution corresponding to each IMF component is over-decomposed

Fig. 5 Time-frequency characteristic diagram of simulation signal over-decomposition verification under white noise interference

In the simulation signal, due to the known signal characteristics, it is found that IMF4 and IMF5 are white noise interference signals. Although the over-decomposition does not cause damage to the effective signal components, it increases the decomposition process and computational loss, which is not conducive to the application in practical engineering problems. For signals with complex components, over-decomposition may lose effective signal content, especially when the signal is de-noised. So the selection of unreasonable noise signal mode separation is easy to cause information loss. Therefore, the optimal K value selection is extremely important and affects the VMD denoising performance. In the empirical analysis, the proposed SVMD can well determine the optimal number of decomposition modes of VMD, and its operation is simple and computationally small.

3 SVMD denoising

3.1 SVMD denoising feature selection

SVMD can reasonably decompose complex acoustic signals containing white noise. And a reasonable number of IMF component signals can be obtained, of which some IMF components are more closely related to the original signal and contain more effective feature information, while some IMF components are less related to the original signal and contain relatively less feature information. Therefore, it is necessary to extract the effective feature information from the original signal and eliminate the interference information brought by the noisy signal.

In order to reasonably select the effective feature components, the Spearman correlation coefficient between each IMF component and the original signal was used as the SVMD denoising IMF feature selection index. $|r_s|$ reflects the correlation between each IMF and the original signal. $|r_s|$ mean data can be defined as the effective IMF component selection threshold λ, and the $|r_s|$ between each IMF component and the original signal is compared with the threshold λ. The IMF components larger than the threshold λ are regarded as effective feature components, but the feature components smaller than the threshold value are eliminated. Its effective IMF component selection threshold λ is defined as

$$\lambda=\frac{1}{K}\sum_{k=1}^{K}|r_s|. \quad (10)$$

Thus based on the correlation analysis, more representative feature components can be selected. The specific steps for selecting the feature components are described as follows.

Step 1 After SVMD adaptive decomposition, the initial K IMF components are obtained.

Step 2 Calculate the correlation coefficient $|r_s|$ between each IMF component and the corresponding original signal, respectively.

Step 3 Calculate the average threshold λ to select the feature components with the help of Eq. (10).

Step 4 The correlation coefficient among each IMF component and the original signal is compared with the threshold λ. The IMF component smaller than the threshold λ is removed, and the IMF component larger than the threshold λ is selected as the feature component.

The optimal decomposition K value of the simulation signal is 5. According to the determined optimal K value, the simulation signal is decomposed into five bandwidth-constrained IMF components, and the corresponding decomposition results are shown in Fig.3. It can be seen that the IMF components obtained by VMD have different time-frequency characteristics, and each IMF component exhibits different information characteristics. The Spearman correlation coefficients among the IMF components and the corresponding original signals are calculated, and the results are shown in Table 4.

Table 4 Spearman correlation coefficient between IMF component of simulation signal and original signal

IMF	Spearman correlation coefficient
1	0.082 5
2	0.102 6
3	0.880 4
4	0.096 1
5	0.451 0

3.2 SVMD denoising performance

The threshold value for selecting feature components is calculated to be 0.322 5 according to Eq. (10). It can be seen from Table 4 that the Spearman correlation coefficients among IMF3, IMF5, and the original signal are greater than the threshold. Therefore, IMF3 and IMF5 can be selected as the characteristic components of the simulation signal, and the effective signal after denoising can be obtained by reconstructing the IMF3 and IMF5 component signals. The short-time Fourier transform (STFT) results of the denoised and reconstructed signals are compared with the original signals. The results are shown in Fig.6.

It can be seen that the noise-containing signal is denoised and reconstructed by SVMD. Afterwards, the white noise can be removed well, and the original signal features can be extracted. It not only removes the white noise in the stationary signal, but also preserves the main information components of the original signal to the greatest extent without losing the effective information of the data.

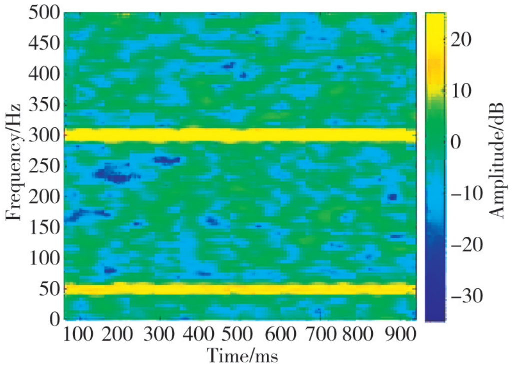

(a) Before denoising

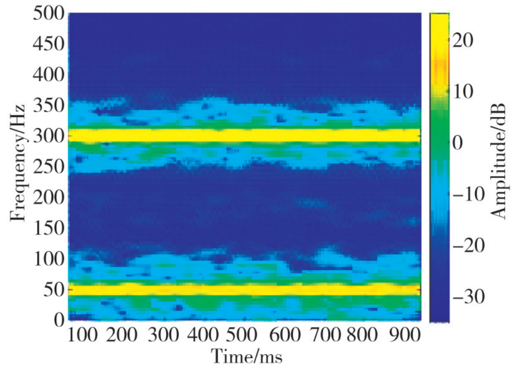

(b) After denoising

Fig. 6 STFT spectrum of simulation signal before and after denoising

To quantitatively describe the denoising effect, signal to noise ratio (SNR) and root mean square error (RMSE) are chosen to quantify the denoising effect. SNR is used to evaluate the denoising effect, and the denoising effect is illustrated by analyzing whether the SNR is improved or not.

$$SNR = 10\lg \frac{\sum_{t=1}^{N} \left| f(t) \right|^2}{\sum_{t=1}^{N} \left| \hat{f}(t) - f(t) \right|^2}, \quad (11)$$

$$RMSE = \sqrt{\frac{\sum_{t=1}^{N} \left| \hat{f}(t) - f(t) \right|^2}{N}}, \quad (12)$$

where $f(t)$ is original signal; $\hat{f}(t)$ is the reconstructed signal after denoising; and N is the signal length.

In general, the larger the SNR after denoising, the smaller the noise mixed in the signal, and the denoising effect is obvious. RMSE represents the difference between the denoised signal and the noise-free signal. The closer the time-domain waveforms are, the better the denoising effect and the smaller the impact on the original signal. White noise signals with different signal-to-noise ratios are added to the simulated signals to generate interference in order to verify the SVMD denoising effect mentioned below for low signal-to-noise environments, after SVMD decomposition and denoising, the signal output signal-to-noise ratio (SNR_{out}) and RMSE parameters in different harsh environments are shown in Table 5.

Table 5 Denoising performance evaluation parameters of signals with different SNR

SNR_{in}/dB	SNR_{out}/dB	RMSE
10	15.800	0.089
5	10.071	0.124
0	4.726	0.186
−5	−0.621	0.215
−10	−5.701	0.232

Comparing the data of various performance indicators after denoising of signals with different signal-to-noise ratios, it is found that the SNR is improved after denoising. It can be removed very well while retaining the original signal characteristics to the greatest extent.

4 SVMD denoising of discharge pulse acoustic signals

In order to verify that the proposed SVMD method has superior denoising performance and high execution efficiency for the measured PD signals, the partial discharge test platform shown in Fig. 7 is built for the white noise interference in the discharge acoustic signals in the low signal-to-noise environment, and the partial discharge pulse acoustic signals are collected. The needle plate electrode structure was designed with reference to the IEC 60243 standard, and the test connection principle of the partial discharge test platform is shown in Fig. 7(a). Fig. 7(b) is a real picture of the simulated fuel tank and electrode support.

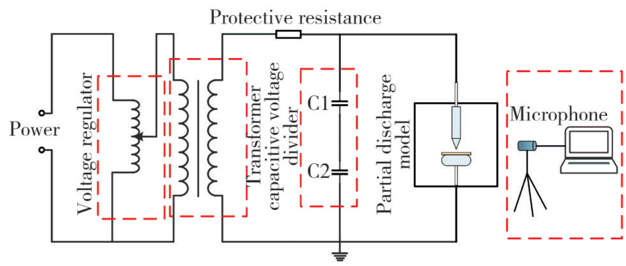

(a) Test wiring schematic

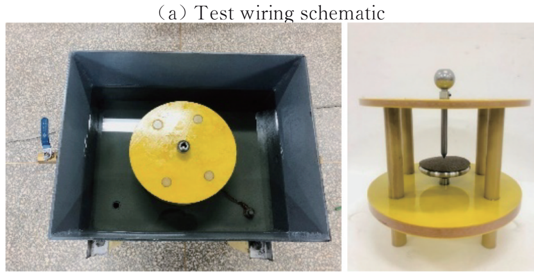

(b) Physical map of simulated fuel tank and electrode support

Fig. 7 Diagrams of partial discharge test

The actual collected discharge acoustic signal waveform is shown in Fig. 8(a). The discharge pulse signal is submerged by a large amount of noise, and the discharge fluctuation cannot be observed well. The signal after SVMD denoising is shown in Fig.8(b), and it is found that the reconstructed signal is perfect. It retains the characteristics of the discharge pulse acoustic signal, can clearly capture the discharge timing, and provides a good signal timing envelope for fault detection.

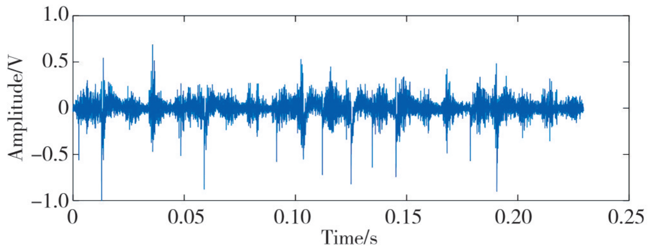

(a) Measured partial discharge acoustic signal

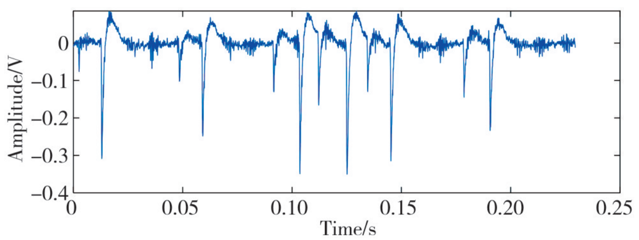

(b) SVMD denoising results

Fig. 8 Partial discharge acoustic signal denoising results

In order to compare the performance of SVMD with traditional denoising methods, the process is very similar to wavelet denoising. Because it needs to consider multi-layer signal decomposition and adaptive filtering. Therefore the soft threshold and hard threshold functions of "rigrsure", "heursure", and "sqtwolog" in wavelet denoising are selected for comparison[23]. Since the discharge pulse signal is mixed with noise signal, its signal-to-noise ratio cannot be determined. In order to unify the parameters, white noise with signal-to-noise ratios of 10 dB, 0 dB, and −10 dB is added to pulse discharge acoustic signal to evaluate its denoising performance.

The performance parameters after SVMD and wavelet denoising are shown in Table 6. H represents the hard threshold and S represents the soft threshold. Since the added white noise signal is generated by random numbers and there are slight differences in each run, the performance evaluation data after denoising is a mean expression of the results of five runs.

Comparing the SNR_{out} and RMSE evaluation parameters, it is found that the performance parameters of SVMD after denoising are better than the traditional wavelet threshold denoising method. The signal-to-noise ratio becomes larger and the noise signal interference is reduced. The original signal characteristics are retained as much as possible in the denoising process. Its error is reduced without affecting the original signal characteristics. And the signal is smoother after denoising, which can effectively extract the discharge pulse timing characteristics. Therefore, the proposed SVMD method can be well applied to the study of partial discharge pulse acoustic signal and is suitable for white noise processing in transformer partial discharge acoustic signal.

Table 6 Measured PD signal denoising performance parameters

Parameter	SNR_{out}/dB			RMSE		
SNR_{in}/dB	10	0	−10	10	0	−10
Sqtwolog+H	5.969	4.531	0.313	0.029	0.034	0.050
Sqtwolog+S	5.146	3.918	0.187	0.032	0.037	0.050
Rigrsure+H	11.521	5.581	0.473	0.014	0.030	0.087
Rigrsure+S	9.623	6.356	−1.24	0.018	0.028	0.050
Heursure+H	6.772	4.986	0.416	0.026	0.032	0.049
Heursure+S	5.455	4.143	0.271	0.031	0.036	0.050
SVMD	12.198	6.952	1.204	0.012	0.021	0.039

5 Conclusions

The VMD decomposition method based on the Spearman correlation coefficient could adaptively and reasonably decompose the complex acoustic signal, extract the characteristics of each modal component of the original signal, and avoid the modal mixing and modal redundancy problems in the traditional VMD decomposition.

Based on the correlation coefficient between each IMF component after SVMD decomposition, the correlation of each mode after traditional VMD decomposition could be tested, and the optimal mode number K value could be optimized. The average threshold of correlation coefficient could eliminate the interference components in each IMF component after SVMD decomposition, and effectively remove white noise interference.

SVMD is a new adaptive denoising method with better white noise signal suppression performance than the traditional wavelet thresholding method. It could retain the original discharge pulse timing characteristics to the maximum extent while effectively removing white noise.

Acknowledgement

This work was supported by State Grid Gansu Electric

Power Research Institute (No.52272219000Q).

Declaration of conflicting interests

The authors have no conflict of interests related to this publication.

References

[1] TANG Z G, TANG M Z, LI J Z, et al. Review on partial discharge pattern recognition of electrical equipment. High Voltage Engineering, 2017, 43(7): 2263-2277.

[2] LÜ F C, NIU L L, WANG S H, et al. Discharge severity assessment of porcelain suspension insulators based on UV images and improved YOLOv3. High Voltage Engineering, 2021, 47(2): 377-386.

[3] XU Z R, YANG L J, WEI Y H, et al. Partial discharge characteristics of fast developing discharge in oil-pressboard insulation. Proceedings of the CSEE, 2021, 41(21): 7529-7540.

[4] WU L P, WU Q, FENG Y, et al. State recognition of transformer based on SVM classification of vibration signals. High Voltage Apparatus, 2019, 55(11): 232-238.

[5] YE B, ZHOU K, HUANG Y L, et al. A white nosie suppression method for partial discharge based on AWM and OSVD. Proceedings of the CSEE, 2021, 41(11): 3978-3987.

[6] YU H, ZHUANG C J, ZENG R, et al. Adaptive wavelet de-noising method for improving the accuracy of transient overvoltage measurement. High Voltage Engineering, 2020, 46(6): 2139-2147.

[7] YANG Y. Fault diagnosis of reduction gear box based on EMD and wavelet analysis. Chengdu: Southwest Jiaotong University, 2020.

[8] DRAGOMIRETSKIY K, ZOSSO D. Variational mode decomposition. IEEE Transactions on Signal Processing, 2014, 62(3): 531-544.

[9] SMRUTHY A, SUCHETHA M. Real-time classification of healthy and apnea subjects using ECG signals with variational mode decomposition. IEEE Sensors Journal, 2017, 17(10): 3092-3099.

[10] XUE Y J, CAO J X, WANG D X, et al. Application of the variational-mode decomposition for seismic time – frequency analysis. IEEE Journal of Selected Topics in Applied Earth Observations and Remote Sensing, 2016, 9(8): 3821-3831.

[11] GAO Z Y, WANG X F, LIN J, et al. Online evaluation of metal burn degrees based on acoustic emission and variational mode decomposition. Measurement, 2017, 103: 302-310.

[12] LI F Y, ZHANG B, VERMA S, et al. Seismic signal denoising using thresholded variational mode decomposition. Exploration Geophysics, 2018, 49(4): 450-461.

[13] LEI Z F, LEI X F, ZHOU C H, et al. Research on feature extraction of ship-radiated noise based on compressed sensing and center frequency. IEEE Access, 2021, 9: 128679-128686.

[14] WU W X, WANG Z J, ZHANG J P, et al. Research of the method of determining K value in VMD based on kurtosis. Journal of Mechanical Transmission, 2018, 42(8): 153-157.

[15] AO Y F, LI H, ZHANG J G, et al. Rocket engine turbopump condition monitoring method based on VMD and FCM. Journal of Test and Measurement Technology, 2024, 38(5): 527-534.

[16] LI Y X, LI Y A, CHEN X, et al. Research on ship-radiated noise denoising using secondary variational mode decomposition and correlation coefficient. Sensors, 2017, 18(1): 48.

[17] ZHANG X, MIAO Q, ZHANG H, et al. A parameter-adaptive VMD method based on grasshopper optimization algorithm to analyze vibration signals from rotating machinery. Mechanical Systems and Signal Processing, 2018, 108: 58-72.

[18] HE Y, WANG H, GU S. New fault diagnosis approach for bearings based on parameter optimized VMD and genetic algorithm. Journal of Vibration and Shock, 2021, 40(6): 184-189.

[19] FU X Y. Research on fault diagnosis of gearbox based on VMD and extreme learning machine. Tianjin: Hebei University of Technology, 2020.

[20] WANG R. Research on gear fault diagnosis method based on ABC-VMD and random forest. Jiangsu: Nanjing University of Information Technology, 2019.

[21] JIA K, YANG Z, WEI C, et al. Pilot protection based on spearman rank correlation coefficient for transmission line connected to renewable energy source. Automation of Electric Power Systems, 2020, 44(15): 103-111.

[22] SONG H Y, PARK S. An analysis of correlation between personality and visiting place using Spearman's rank correlation coefficient. KSII Transactions on Internet and Information Systems, 2020, 14(5): 1951-1966.

[23] SRIVASTAVA M, LINDSAY ANDERSON C, FREED J H. A new wavelet denoising method for selecting decomposition levels and noise thresholds. IEEE Access, 2016, 4: 3862-3877.

基于改进VMD的油中典型电极放电声信号去噪

曹盘盘[1], 马建桥[1*], 杨广泽[1], 冯婷娜[2], 王 鑫[3]

1. 兰州交通大学 自动化与电气工程学院, 甘肃 兰州 730070;
2. 国网新疆电力有限公司 哈密供电公司, 新疆 哈密 839000;
3. 内蒙古电力(集团)有限责任公司 包头供电局, 内蒙古 包头 014030

摘 要: 白噪声易对变压器局部放电(Partial discharge, PD)声信号造成强烈干扰, 严重影响放电故障识别及监测效果。为抑制局部放电检测中存在的白噪声干扰及准确提取强噪声环境下变压器局部放电脉冲声信号特征, 本文深入分析了低信噪比(Signal-to-noise ratio, SNR)环境下放电脉冲声信号的自适应性分离与去噪。首先, 基于Spearman相关系数确定了变分模态分解(Variational mode decomposition, VMD)的最佳分解模式数 K。然后, 通过模拟信号验证了所提SVMD(Spearman-variational mode decomposition, SVMD)方法分解的可靠性。最后, 基于Spearman相关系数平均阈值法对实际放电脉冲声信号分解去噪, 提取放电脉冲信号本征模态函数分量。结果表明, SVMD可自适应性地解决VMD模式数未知缺陷, 能够有效提取复杂信号中的有效模态分量, 可成功实现变压器局部放电声信号的去噪。该方法可有效去除局部放电声信号中的白噪声干扰, 并获得平滑的滤波信号, 最大程度地保留了PD信号的完整性, 有利于对其进行后续研究, 对VMD的改进有助于推进其在工业设备状态巡检中的广泛使用。

关键词: 故障识别; Spearman相关系数; 变分模态分解(VMD); 局部放电; 声信号

引用格式: CAO Panpan, MA Jianqiao, YANG Guangze, et al. Typical electrode discharge acoustic signal denoising in oil based on improved VMD. Journal of Measurement Science and Instrumentation, 2025, 16(2): 224-235. DOI: 10.62756/jmsi.1674-8042.2025022